# Dalton Transactions



# **PAPER**



**Cite this:** *Dalton Trans.*, 2021, **50**, 15296

# Di(hydroperoxy)adamantane adducts: synthesis, characterization and application as oxidizers for the direct esterification of aldehydes†

Fabian F. Arp, (1) ‡ Rahym Ashirov, (1) ‡ Nattamai Bhuvanesh and Janet Blümel (1) \*

The di(hydroperoxy)adamantane adducts of water (**1**) and phosphine oxides  $p\text{-}Tol_3PO\text{-}(HOO)_2C(C_9H_{14})$  (**2**),  $o\text{-}Tol_3PO\text{-}(HOO)_2C(C_9H_{14})$  (**3**), and  $Cy_3PO\text{-}(HOO)_2C(C_9H_{14})$  (**4**), as well as a  $CH_2Cl_2$  adduct of a phosphole oxide dimer (**8**), have been created and investigated by multinuclear NMR spectroscopy, and by Raman and IR spectroscopy. The single crystal X-ray structures for **1–4** and **8** are reported. The IR and <sup>31</sup>P NMR data are in accordance with strong hydrogen bonding of the di(hydroperoxy)adamantane adducts. The Raman  $\nu(O-O)$  stretching bands of **1–4** prove that the peroxo groups are present in the solids. Selected di(hydroperoxy)alkane adducts, in combination with AlCl<sub>3</sub> as catalyst, have been applied for the direct oxidative esterification of n-nonyl aldehyde, benzaldehyde, p-methylbenzaldehyde, p-bromobenzaldehyde, and o-hydroxybenzaldehyde to the corresponding methyl esters. The esterification takes place in an inert atmosphere, under anhydrous and oxygen-free conditions, within a time frame of 45 minutes to 5 hours at room temperature. Hereby, two oxygen atoms per adduct assembly are active with respect to the quantitative transformation of the aldehyde into the ester.

Received 24th September 2021, Accepted 30th September 2021 DOI: 10.1039/d1dt03243a

rsc.li/dalton

## 1. Introduction

One of the most important substance classes in academia, industry, and in the household are peroxides. Consequently, crystalline peroxosolvates have enjoyed an exponential growth in interest over the last decade.2 Peroxides are active ingredients for bleaching in the production of goods, for wastewater treatment, and for disinfection<sup>1,2</sup> in the household and in medicine, for radical-initiated polymerizations, 1b and disintegrating the novel corona virus. Peroxides are also important for oxidation reactions, with or without supporting catalysts. 1,2 For example, amines are oxidized to obtain amides,3 and alkanes can be activated.4 Epoxidations rely on favorable oxidizers,5 and sulfides can be transformed selectively into sulfoxides.6 Even the clean oxidation of phosphines to phosphine oxides is a non-trivial task.7-11 Other examples include the Baeyer-Villiger oxidation for transforming ketones into lactones, 12 and the direct formation of esters from aldehydes 13-28

Department of Chemistry, Texas A&M University, College Station, TX, 77842-3012,

‡Both authors contributed equally to the manuscript.

USA. E-mail: bluemel@tamu.edu; Fax: +1 979-845-5629

can be accomplished by using peroxides in combination with transition metal catalysts.  $^{21-28}$ 

Aqueous  $H_2O_2$  is ubiquitous, but not an ideal oxidizing reagent. Its major drawback is the abundance of water it brings into the reaction mixture, which often leads to unwanted secondary reactions. Furthermore, aqueous  $H_2O_2$  has to be titrated<sup>29</sup> prior to each application when exact stoichiometry is needed. In case the reagents are not water soluble the oxidation reactions have to be performed in a biphasic system, slowing rates and requiring phase separations later. Water-free formulations of  $H_2O_2$  such as urea hydrogen peroxide (UHP)<sup>30</sup> and peroxocarbonates<sup>31</sup> are used, but their composition is not well defined and they are basically insoluble in organic solvents. Peroxides like  $(Me_3SiO)_2$  and  $(CH_3)_2C(OO)$  (DMDO) are applied, but their synthesis and storage are problematic.<sup>32</sup>

Phosphine oxides play increasingly important roles in synthetic chemistry, as final products or intermediates.<sup>33,34</sup> Their application in Mitsunobu reactions has been described,<sup>34g</sup> and they are attractive organocatalysts for the recently explored redox-free version of this reaction.<sup>34h</sup> Phosphine oxides are also co-products of Wittig and Appel reactions and unwanted byproducts of phosphine chemistry, especially in the field of catalysts immobilized with bifunctional phosphines.<sup>35,36</sup> Phosphine oxides can be used to probe surface acidities<sup>37</sup> and they aid as models in decomposing warfare agents.<sup>38</sup> Most recently, it has been discovered that phosphine oxides self-

<sup>†</sup>Electronic supplementary information (ESI) available: Crystallography data. CCDC 1980801 (1), 1980802 (2), 1980803 (3), 1980804 (4) and 2023784 (8). For ESI and crystallographic data in CIF or other electronic format see DOI: 10.1039/d1dt03243g

adsorb on surfaces in the absence of solvents, and their mobilities have been investigated using NMR in the solid state. <sup>39–41</sup> Importantly, phosphine oxides readily form hydrogen bonds with different donors like phenols to create extended networks. <sup>42–44</sup> Other hydrogen bond donors include naphthol, <sup>44</sup> sulfonic acids, <sup>45</sup> and even water. <sup>41,46,47</sup> Hydrogenbonded motifs have also been reported in combination with silanols and chloroform. <sup>48</sup> The most powerful methods to analyze these diverse P(v) species are multinuclear solid-state NMR and X-ray diffraction. <sup>39–41,48–50</sup>

More recently, our group has worked at creating superior oxidizers by hydrogen-bonding favorable peroxides to phosphine oxides. We communicated two new varieties of phosphine oxide adducts. <sup>51–55</sup> Hilliard adducts  $(R_3PO\cdot H_2O_2)_2$  (R = alkyl, aryl) are generated by treating phosphine oxides or phosphines with  $H_2O_2$ . <sup>11,47,53</sup> When ketones (R'COR") are added, Ahn adducts, di(hydroperoxy)alkane adducts of phosphine oxides,  $R_3PO\cdot (HOO)_2CR'R''$  (R,R',R" = alkyl, aryl), are obtained. <sup>51,52–55</sup>

The studies on Ahn adducts so far allow these statements: (a) All adducts are obtained reproducibly, and with welldefined composition. (b) All adducts crystallize readily in large habits. (c) The structures and packing motifs of Ahn adducts are of a general nature, irrespective of the substituents R, R', and R". (d) All adducts are stable and safe at elevated temperatures, and when being hammered and ground, with shelf lives of months at ambient temperatures. (e) Different synthetic routes starting from the phosphines, their oxides, and from Hilliard adducts can be employed to generate Ahn adducts.<sup>54</sup> (f) In the presence of suitable substrates one Ahn adduct releases two active oxygen atoms in a consecutive manner. 54,55 (g) The high solubility of all adducts in organic solvents allows for oxidation reactions in one homogeneous phase. (h) The reactivity of Ahn adducts matches that of aqueous H<sub>2</sub>O<sub>2</sub>, however, they do not come with an excess of water that may entail unwanted secondary reactions. (i) The adducts can be characterized by X-ray diffraction, Raman and IR spectroscopy, solid-state and solution NMR, including DOSY<sup>51</sup> and natural abundance <sup>17</sup>O NMR. <sup>47,51</sup> (j) Potentially dangerous oligomers like triacetone triperoxide (TATP) have never been found in any preparation, indicating that phosphine oxides efficiently prevent their formation.

The solid Ahn adducts are easy to add to reactions. <sup>47,51–55</sup> The advantage of the anhydrous oxidation has been demonstrated, for example, by the clean synthesis of water-sensitive Ph<sub>2</sub>P(O)P(O)Ph<sub>2</sub>. <sup>55</sup> Sulfides are transformed into sulfoxides in organic phases without overoxidation to the sulfones. <sup>53,54</sup> Baeyer–Villiger oxidations of ketones yield lactones selectively, while requiring mere traces of an acid as a catalyst. <sup>55</sup>

In the presented work Ahn adducts are applied as oxidizers in the direct formation of esters from aldehydes. Esters represent one of the most prevalent functional groups in organic chemistry. They are abundant in various natural products, polymers, and pharmaceuticals.<sup>13</sup> Their omnipresence has motivated chemists to develop different synthetic strategies over the past century. The direct esterification of aldehydes is

conceptually and economically more attractive than traditional methods that are based on acid activation followed by nucleophilic substitution, and therefore receives increasing attention. The main advantages consist of utilizing readily available starting materials and avoiding the isolation of free carboxylic acid intermediates. This can be particularly important in natural product synthesis when incompatible functionalities or protecting groups are present in the substrate.

Numerous direct oxidative esterification methods have been developed, for example, the oxidative esterification of aldehydes *via* hemiacetal intermediates. Direct esterifications of aldehydes by oxidation of hemiacetals without use of a transition metal catalyst have been reported with organic and inorganic oxidants such as iodine, <sup>14</sup> oxone, <sup>15</sup> iodine and diacetoxyiodobenzene, <sup>16</sup> *N*-iodosuccinimide, <sup>17</sup> sodium hypochlorite, <sup>18</sup> pyridinium hydrobromide perbromide, <sup>19</sup> and hydrogen peroxide. <sup>20</sup> However, the instability of the hemiacetal intermediate and steric features of the aldehydes and alcohols are not compatible with the majority of these reagents. Most of the methods yield only methyl esters or they are applicable only with very reactive aromatic aldehydes.

So far, most successful are transition metal-catalyzed oxidative esterifications. <sup>21–28</sup> For example, oxidative esterifications of aldehydes were achieved by using rhodium-,21 vanadium-,22 palladium-,<sup>23</sup> gold-,<sup>24</sup> iron-,<sup>25</sup> and copper-based<sup>26</sup> catalysts. The main drawbacks of these methods are the unfavorable stoichiometric ratios of the reagents, limited substrate scope, and the harsh reaction conditions needed. Moreover, largescale use of these methods is not practical because of the catalyst cost. An alternative strategy for the oxidative esterification of aldehydes that does not involve the formation of hemiacetals is the oxidative esterification of aldehydes by using N-heterocyclic carbenes (NHC) as catalysts. 27,28 Examples of metal-free NHC-catalyzed<sup>27</sup> and NHC transition-metal-catalyzed<sup>28</sup> esterifications have been reported. Unfortunately, these methods are not generally applicable and have been optimized for either aromatic or aliphatic aldehydes. Furthermore, a large excess of primary alcohols is needed. Most recently, however, the successful NHC/carboxylic acid co-catalysis for the oxidative esterification of demanding aldehydes has been communicated.56

In this contribution we pursue three goals. First, we seek to broaden the range of ketones that can be used to create di(hydroperoxy)alkanes. It is demonstrated that not only ketones flanked by two n-alkane groups can form Ahn adducts, but also the sterically demanding adamantanone with two tertiary carbon atoms bound to the carbonyl group (Fig. 1). Second, we report an attempt to use a phosphole oxide as stabilizing carrier for Ahn adducts. While the desired Ahn adduct could not be generated, the attempt led to the discovery of an easy stereoselective synthesis of a phosphole dimer that could also be characterized by single crystal X-ray diffraction. Finally, the general applicability of Ahn adducts as oxidizers for the direct oxidative esterification of several aliphatic and aromatic aldehydes is demonstrated. Hereby, the inexpensive AlCl<sub>3</sub> can be used as the catalyst under anhydrous conditions.

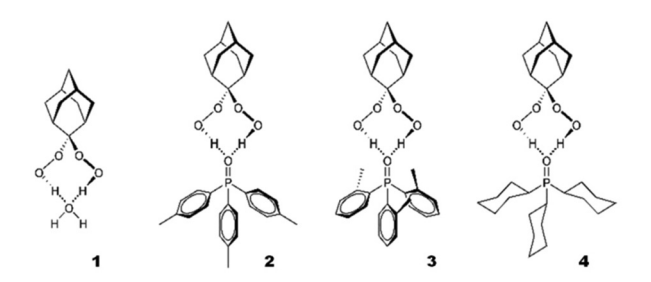


Fig. 1 Di(hydroperoxy)adamantane adducts of water,  $H_2O\cdot(HOO)_2C$  ( $C_9H_{14}$ ) (1), and phosphine oxides,  $p\text{-}Tol_3PO\cdot(HOO)_2C(C_9H_{14})$  (2),  $o\text{-}Tol_3PO\cdot(HOO)_2C(C_9H_{14})$  (3), and  $Cy_3PO\cdot(HOO)_2C(C_9H_{14})$  (4).

Therewith, the scope of oxidizing agents and catalysts for the oxidative esterification of aldehydes will be broadened. This synthetic approach is an attractive alternative to the currently used methods because it does not require a transition metal, it works at room temperature, is fast and uses an inexpensive, non-toxic catalyst.

# 2. Results and discussion

#### 2.1. Synthesis and purification

In order to broaden the range of well-characterized peroxides with reproducible composition, several new Ahn adducts incorporating peroxo groups have been created (Fig. 1). Hereby, special emphasis has been placed on the selection of a strained ketone to probe the boundaries of adduct formation. Furthermore, the ketone-derived di(hydroperoxy)-adamantane moiety in 1-4 is the same, so the influence of the different phosphine oxides on the adduct characteristics can be investigated systematically. The water adduct of di(hydroperoxy)adamantane (1) has been synthesized by reacting adamantanone with aqueous H2O2 in the presence of iodine as the catalyst.<sup>57</sup> Since di(hydroperoxy)adamantane is more strongly hydrogen-bonded to phosphine oxides than to water, the Ahn adducts 2-4 are accessible by reaction of 1 with the corresponding phosphine oxides p-Tol<sub>3</sub>P=O (5), o-Tol<sub>3</sub>P=O (6), and  $Cy_3P = O(7)$ .

An attempt to probe the boundaries of the range of applicable phosphine oxide carriers by using 1,2,5-triphenylphosphole leads via 2 + 2 cycloaddition to the stereoselective formation of the phosphole oxide dimer 8 in a high yield. Interestingly, instead of hydrogen-bonded hydroperoxy groups or  $H_2O_2$ , dichloromethane (DCM) has been incorporated in the solid-state structure in a bridging function. Other approaches aimed at reducing the weight of the phosphine oxide carrier have been based on the secondary phosphine  $HPPh_2$  and  $HP(O)Ph_2$ . However, phosphinic acid has been retrieved quantitatively from each experiment performed under varied conditions.

All adducts crystallize readily in large specimens and can be purified by recrystallization. This feature, together with their high solubility in organic solvents, facilitates the characterization. Especially meaningful for the new adducts are Raman and IR spectroscopy, as well as single crystal X-ray diffraction and NMR analyses. The shelf life of adamantane-based Ahn adducts matches that reported earlier. For example, polycrystalline (o-Tol)<sub>3</sub>P=O·(HOO)<sub>2</sub>C(CH<sub>3</sub>)<sub>2</sub> retains 88% oxidative power after being stored in the freezer for one year at -20 °C.

#### 2.2. Single crystal X-Ray diffraction

The species 1–4 can easily be obtained in large colorless habits, therefore they have been investigated by single crystal X-ray diffraction (Fig. 2, 3 and 4). The structure of the phosphole oxide dimer 8 is displayed in Fig. S1† and 5. Most probably the phosphine oxide carriers help 2–4 to crystallize. All P=O bond lengths are summarized in Table 1, the O···H and oxygen-oxygen distances in the moieties O···H–O in Table 2. The dihedral angles C-C-P=O and O···O-O-C are reported in Table 3.



Fig. 2 Single crystal X-ray structure of H<sub>2</sub>O·(HOO)<sub>2</sub>C(C<sub>9</sub>H<sub>14</sub>) (1).<sup>58</sup>

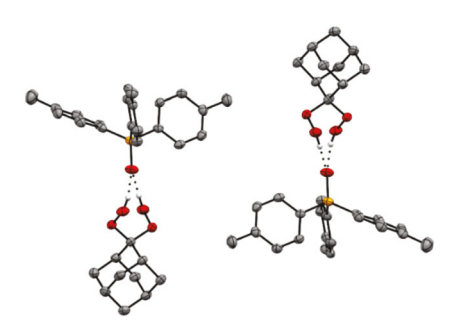


Fig. 3 X-Ray structure of two independent adducts units of  $p\text{-Tol}_3\text{PO}\cdot(\text{HOO})_2\text{C(C}_9\text{H}_{14})$  (2).  $^{58}$ 

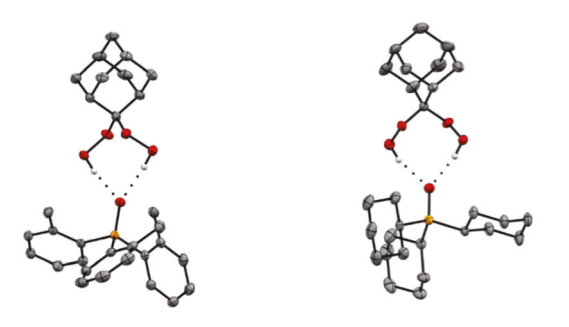
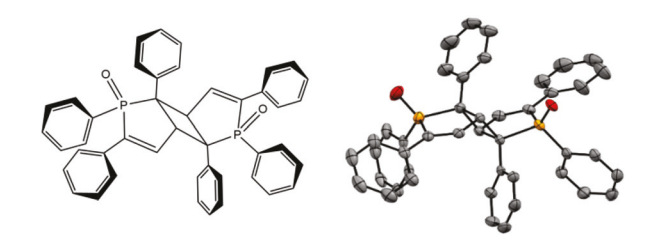


Fig. 4 X-Ray structures of o-Tol<sub>3</sub>PO·(HOO)<sub>2</sub>C(C<sub>9</sub>H<sub>14</sub>) (3, left) and Cy<sub>3</sub>PO·(HOO)<sub>2</sub>C(C<sub>9</sub>H<sub>14</sub>) (4, right).<sup>58</sup>



**Fig. 5** Single crystal X-ray structure of the phosphole oxide dimer DCM adduct **8**. The DCM molecules and H atoms are not displayed for clarity.<sup>58</sup>

**Table 1** P=O bond lengths (Å) of the adducts **2–4**,<sup>58</sup> compared with the bond lengths of the corresponding pure phosphine oxides, and the differences  $\Delta(P=O)$  of the bond lengths

Adduct	Adduct P=O bond lengths (Å)	R₃PO P≕O lengths (Å)	Δ(P=O) (Å)
2 3	1.5005(12) 1.4984(10)	1.4885(17) (ref. 51) 1.478(2)/1.481(2) (ref. 59)	0.012 0.0204/0.0174
4	1.5077(11)	1.486/1.489/1.490 (ref. 60)	0.0217/0.0187/ 0.0177

Table 2  $H_2O\cdots H$  (1) and  $PO\cdots H$  (2-4), and oxygen-oxygen distances  $O\cdots H-O$  (Å) of the adducts  $1-4^{58}$ 

Adduct	O…H distances (Å)	O···H–O distances (Å)
1	1.750/1.862	2.6611(14)/2.8080(15)
2	1.865/1.917	2.69(2)/2.748(10)
3	1.867/1.939	2.712(3)/2.781(4)
4	1.846/1.887	2.680(7)/2.706(7)

Table 3 Dihedral angles (°) in the di(hydroperoxy)adamantane adducts  $1-4^{58}$ 

Adduct	C-O-O···O	O=P-C-C
1 2 3 4	92.75(9)/96.47(9) -88.5(3)/-100.2(3) 92.73(12)/95.09(12) 93.03(19)/93.15(18)	

In the water adduct of di(hydroperoxy)adamantane (1) the peroxo molecules are connected with each other *via* the hydrogen-bonded water, hereby forming an extended two-dimensional network. Interestingly, even with this new structural motif, two neighboring adamantane moieties are oriented in opposite directions, like in the hydrogen-bonded assemblies with phosphine oxides.

The phosphine oxide/di(hydroperoxy)adamantane assemblies in 2–4 each exhibit two geminal HOO groups bound to the O=P function (Fig. 3 and 4). This structural motif has been communicated previously for other Ahn adducts. <sup>51–55</sup> Therefore, 2–4 corroborate the general structural nature and exact stoichiometry with two hydrogen bonds per O=P group.

Each phosphine oxide group carries two active oxygen atoms, one more per assembly than Hilliard adducts. 11,47,53 All adducts of 2–4 are arranged so that adjacent ones point in opposite directions, as shown for 2 (Fig. 3).

In all adducts 2-4 the P=O bonds are longer than those of the corresponding phosphine oxides by 0.012 to 0.0217 Å (Table 1). The P=O bonds in 2-4 are longer because hydrogen bonding to the HOO groups renders them weaker. IR spectroscopy corroborates these results (see below). Comparing the two adducts with triarylphosphine oxide carriers, 2 and 3, the P=O bonds are more elongated for the ortho methyl substituted species than for the para-substituted version. The structure of 3 does not show steric congestion, therefore electronic effects might dominate the length of the P=O bond in this case. The largest P=O bond length difference with 0.017 Å can be found for 4 which incorporates the Cy<sub>3</sub>PO carrier. This result is expected, as it has been demonstrated with dynamic NMR spectroscopy earlier that this phosphine oxide binds more strongly to di(hydroperoxy)alkanes than triarylphosphine oxides.51

All O···H distances in the structures of the adducts,  $H_2O$ ···H in 1 and PO···H in 2–4, are between 1.750 and 1.939 Å (Table 2). According to the literature, hydrogen bonds typically exhibit O···H distances of 1.85 to 1.95 Å. Therefore, it can be concluded that all di(hydroperoxy)adamantane adducts form strong hydrogen bonds to water and phosphine oxides.

Furthermore, the oxygen-oxygen O···H–O distances, which can be regarded as another indicator for the formation of hydrogen bonds, <sup>62</sup> all lie within the range of 2.661–2.808 Å in **1–4** (Table 2), which is again well within the established 2.75–2.85 Å region for O···H–O. <sup>62</sup>

Another interesting feature of Ahn adducts are the C-O-O···O dihedral angles. For 1–4 (Table 3) it is found that at least one of the hydrogen bonds per adduct exhibits an absolute value in the range from 88.5° to 93.03°. In comparison, solid hydrogen peroxide has a dihedral angle of 90.2(6)°. The second hydrogen bond of each assembly in 1–4 shows a higher degree of distortion, most probably to allow for arrangement in the crystal. These dihedral angles assume values from 93.15° to 100.2° (Table 3).

Contemplating the O=P-C-C dihedral angles of 2-4 is interesting in the context of a recent theoretical study of phenyl ring conformations in Ph<sub>3</sub>PO.<sup>63</sup> Based on this study, the minima with respect to energy of the O=P-C-C dihedral angle lie around ±33° and ±25° of 0° or 180°, as determined by different theoretical methods. Assessing dihedral angles in Ph<sub>3</sub>PO moieties from crystal structures of species without metals, they are clustering in the areas of ±15-30° around 0° and 180°.63 Adducts 2 and 3 are perfect candidates to test this theory using the O=P-C-C dihedral angles (Table 3). Obviously, the steric demand of the methyl groups in the ortho positions of the phenyl rings in 3 lead to a large deviation from both calculations and experimentally predicted values. The O=P-C-C dihedral angles in 3 are larger than those in Ph<sub>3</sub>PO. In 2, the para methyl groups do not exert steric strain and therefore the dihedral angles follow the calculated and

experimentally found ranges.<sup>63</sup> For completeness, Table 3 also includes the dihedral O=P-C-C angles of 4 which shows the characteristic chair conformation of the cyclohexyl rings.

The desire to decrease the weight and to broaden the range of applicable phosphine oxide carriers provoked the treatment of 1,2,5-triphenylphosphole with the water adduct of di(hydroperoxy)adamantane 1. Instead of the expected phosphole oxide adduct, however, a 2 + 2 cycloaddition takes place, and the dimer 8 is obtained in high yield (Fig. S1† and 5). The 1,2,5-triphenylphosphole dimer has previously been obtained by irradiation. Although it is not the desired product, the structure of 8 incorporates interesting features. The stereochemistry is in analogy to the reported dimer. The two P=O groups in the molecule are pointing to the same side of the ring system (Fig. 5).

Another interesting aspect of the X-ray structure of 8 is the presence of two bridging DCM molecules between two molecules of 8 (Fig. S1†). Hydrogen bonding between P=O and HO groups is a classic type. However, P=O groups can also form hydrogen bonds in the presence of polarized C-H bonds, and several structures of phosphine oxides with hydrogen-bonded CHCl<sub>3</sub> have been reported. Hese cases, each P=O group interacts with one CHCl<sub>3</sub> hydrogen. In the crystal of 8, however, two hydrogen bonds to P=O groups are formed by each bridging DCM molecule (Fig. S1†).

#### 2.3. <sup>31</sup>P NMR spectroscopy

The solubilities of 2-4 are high in the conventional solvents, in accordance with the solubilities of other Ahn adducts.<sup>51–55</sup> <sup>31</sup>P NMR spectroscopy is the analytical method of choice and spectra are obtained within minutes. In order to avoid cumbersome external referencing and altering the chemical shifts by an internal standard, it is inserted in a capillary. The chemical shifts of 2-4 assume 2.36 to 8.13 ppm higher values than the corresponding pure phosphine oxides  $p\text{-Tol}_3P=O$  (5), o-Tol<sub>3</sub>P=O (6), and Cy<sub>3</sub>P=O (7) (Table 4). This observation is in accordance with values from other Ahn adducts.51-55 The higher chemical shift values are due to interactions with the HOO groups, which lead to deshielding of the <sup>31</sup>P nuclei. The electron densities are drawn towards the oxygen atoms in the P=O groups. Therefore, the <sup>31</sup>P NMR signals of Ahn<sup>51-55</sup> and Hilliard adducts<sup>11,47,53</sup> are shifted downfield. A higher  $\Delta\delta(^{31}P)$ value indicates stronger hydrogen bonding. Therefore, it can be concluded that the trialkylphosphine oxide  $Cy_3P=O$  (7) binds most firmly, followed by the triarylphosphine oxide

Table 4  $^{31}$ P NMR chemical shifts of the adducts 2–4 and their corresponding phosphine oxides 5–7 in CDCl<sub>3</sub> and the differences  $\Delta\delta(^{31}$ P) of the chemical shift values

Adduct	$\delta(^{31}P)$ of adducts [ppm]	$\delta$ ( $^{31}$ P) of R <sub>3</sub> PO [ppm]	$\Delta\delta(^{31}P)$ [ppm]
2	32.30	29.28 (ref. 47)	3.02
3	39.87	37.51 (ref. 47)	2.36
4	58.04	49.91 (ref. 11)	8.13

 $p ext{-}\mathrm{Tol}_3\mathrm{P} = \mathrm{O}$  (5). The phosphine oxide  $o ext{-}\mathrm{Tol}_3\mathrm{P} = \mathrm{O}$  (6) is most weakly bound. The IR data discussed below and exchange experiments reported earlier corroborate this interpretation.

In contrast to the <sup>31</sup>P chemical shifts, there are only minimal changes in the <sup>1</sup>H and <sup>13</sup>C NMR data when creating the Ahn adducts **2–4** from the phosphine oxides **5–7**. This can, for example, be seen when comparing the  $\delta(^{13}\text{C})$  and  $I(^{31}\text{P}-^{13}\text{C})$  values of **2** with those of **5**.<sup>51</sup>

#### 2.4. IR and Raman spectroscopy

The Ahn adducts 1-4 incorporate two functional groups that are meaningful for the characterization by IR spectroscopy,<sup>67</sup> P=O, and O-H. The stretching frequencies of the P=O groups can be compared with those of the corresponding pure phosphine oxides p-Tol<sub>3</sub>P=O (5), o-Tol<sub>3</sub>P=O (6), and Cy<sub>3</sub>P=O (7). The  $\nu(P=0)$  of 1-4 are 5-56 cm<sup>-1</sup> smaller than those of the neat phosphine oxides 5-7. As discussed above in the <sup>31</sup>P NMR section, the interactions of the HOO groups with the P=O oxygen weaken this bond and reduce the wavenumbers. The differences range between 5-56 cm<sup>-1</sup> (Table 5), which is in general in accordance with earlier studies of Ahn adducts with phosphine oxide carriers. 51-55 Interestingly, the extent of the weakening of the P=O group by the hydrogen bonding in the Ahn adducts is dominated by the substituents R in the phosphine oxides R<sub>3</sub>PO, while the nature of the di(hydroperoxy) alkane does not play a major role. For example, hydrogen bonding to p-Tol<sub>3</sub>P=O (5) entails a smaller wavenumber  $\nu(P=O)$  in 2 ( $\Delta\nu(P=O) = 32 \text{ cm}^{-1}$ ), which is close to the value observed for the di(hydroperoxy)cyclohexane and -heptane adducts of tri(para-tolyl)phosphine oxide ( $\Delta \nu$ (P=O) = 35 cm<sup>-1</sup> for both).<sup>51</sup> In contrast, the phosphine oxide carrier o-Tol<sub>3</sub>P=O (6) leads to the weakest hydrogen bonding with a low  $\Delta\nu(P=0)$  of 5 cm<sup>-1</sup>, a value that is very close to the 6 cm<sup>-1</sup> reported for  $o\text{-Tol}_3\text{PO}\cdot(\text{HOO})_2\text{C}(\text{CH}_2)_6$ . Finally, the  $\Delta\nu(\text{P=O})$ value for 4 is highest with 56 cm<sup>-1</sup>, which is comparable to the 44 cm<sup>-1</sup> for the di(hydroperoxy)cyclohexane adduct of tricyclophosphine oxide.<sup>54</sup> These results corroborate the assumption that Cy<sub>3</sub>PO (7) interacts more strongly with HOO groups than triarylphosphine oxides. This is in accordance with an earlier

**Table 5** IR stretching frequencies  $\nu(P=O)$  [cm<sup>-1</sup>] of the P=O groups of the di(hydroperoxy)adamantane adducts **1–4** and comparison with their corresponding neat phosphine oxides p-Tol<sub>3</sub>P=O (**5**), o-Tol<sub>3</sub>P=O (**6**), and Cy<sub>3</sub>P=O (**7**),  $\Delta\nu(P=O)$  [cm<sup>-1</sup>],  $\nu(O-H)$  of the hydrogen-bonded hydroperoxy groups, and the Raman  $\nu(O-O)$  stretching frequencies

Adduct	Adduct $\nu(P=O)$ [cm <sup>-1</sup> ]	$R_3PO$ $\nu(P=O)$ $[cm^{-1}]$	$\Delta \nu (P = O)$ [cm <sup>-1</sup> ]	$\nu$ (O–H) of adducts [cm <sup>-1</sup> ]	ν(O-O) [cm <sup>-1</sup> ]
1	_	_	_	3339 <sup>a</sup>	871
2	1153	1185 (ref. 47)	32	3269	869
3	1153	1158 (ref. 47)	5	3296	869
4	1101	1157 (ref. 11)	56	3225	871

 $<sup>^{</sup>a}\nu(O-H) = 3433 \text{ cm}^{-1} (H_{2}O); \nu(O-H) = 1659 \text{ cm}^{-1} (\text{overtone}, H_{2}O).$ 

study of activation enthalpies, performed by studying adduct exchange with dynamic NMR spectroscopy. Regarding the triarylphosphine oxides, IR proves that p-Tol<sub>3</sub>PO is more strongly bound to di(hydroperoxy)alkanes than o-Tol<sub>3</sub>PO, again in perfect harmony with the earlier exchange studies (Table 5).

The wavenumbers  $\nu(\text{O-H})$  of the HOO groups of 1-4 are found within the range of 3339–3225 cm<sup>-1</sup> (Table 5). Additionally, for the water adduct 1, the  $\nu(\text{O-H})$  stretching band of water is discernible at 3433 cm<sup>-1</sup>. The influence of the P=O group on the O-H hydrogen atoms renders the O-H bonds weaker, in this way diminishing the  $\nu(\text{O-H})$  values. In accordance with the scenario of  $\Delta\nu(\text{P=O})$ , the  $\Delta\nu(\text{O-H})$  indicate that Cy<sub>3</sub>P=O leads to the strongest hydrogen bond, followed by  $p\text{-Tol}_3\text{P}$ =O and  $o\text{-Tol}_3\text{P}$ =O, while the hydrogenbonding to water is comparatively weak. Again, these results are in accordance with the  $^{31}\text{P}$  NMR data discussed above and earlier exchange studies.  $^{51}$ 

The adducts 1-4 are symmetric and their Raman spectra have well-defined  $\nu(O-O)$  stretches (Table 5), although they are not as intense as those of the Hilliard adducts. The  $\nu$ (O-O) lie between 869 and 871 cm<sup>-1</sup>, in accordance with the values of analogous adducts<sup>47,51</sup> and with (Ph<sub>3</sub>PO·H<sub>2</sub>O<sub>2</sub>)<sub>2</sub>.68 According to expectation, the bond order is one and consequently the wavenumbers are much lower than those found for  $O_2$  gas  $(1556 \text{ cm}^{-1})^{69}$  and  $O_2^ (1139 \text{ cm}^{-1})^{.70}$  Basically, the ν(O-O) values for the hydrogen-bonded di(hydroperoxy)adamantanes 1-4 lie in the region of aqueous (99.5%) H<sub>2</sub>O<sub>2</sub>  $(880 \text{ cm}^{-1})^{71}$  and  $H_2O_2$  vapor  $(864 \text{ cm}^{-1})^{.72}$  The O-O bonds in 1-4 are, however, still stronger than those in alkali peroxides (736-790 cm<sup>-1</sup>)<sup>73</sup> and in the oxidizing agent <sup>t</sup>BuOOH (847 cm<sup>-1</sup>).<sup>74</sup> In summary, the  $\nu$ (O–O) of 1–4, in combination with the results of the X-ray diffraction studies, prove that peroxo groups are present in the adducts.

#### 2.5. Oxidative direct esterification of aldehydes

In this section, the novel oxidative esterification of aldehydes using Ahn adducts is presented. This is an attractive alternative to the current methods described in the introduction section because it (a) does not require a transition metal, (b) works at room temperature, (c) is fast and (d) uses an inexpensive, non-toxic catalyst (Scheme 1). The Ahn adducts 2-4 can be used to transform nonyl aldehyde to the corresponding methyl ester by reaction with methanol in the presence of AlCl<sub>3</sub>. The reaction progress was monitored by observing the α-CH<sub>2</sub> protons of the relevant species, the aldehyde, acid, and ester by <sup>1</sup>H NMR spectroscopy. These protons have sufficiently different chemical shifts in CDCl<sub>3</sub> (2.41, 2.35, and 2.30 ppm, respectively), so that the ratios of the reaction products can be obtained by integration. In order to avoid signal overlaps with the formed adamantanone from 2-4, the Ahn adduct Ph<sub>3</sub>PO·(HOO)<sub>2</sub>CMe<sub>2</sub> (9)<sup>53</sup> has been employed for a detailed investigating the direct esterification. For analyzing the reaction outcomes for aromatic aldehydes, the corresponding ortho protons of the aldehydes and esters were used.

In a first step, an inexpensive, readily available, effective catalyst was sought. Commercially available  $AlCl_3$  proved to be

**Scheme 1** Direct oxidative esterification of nonyl aldehyde ( $R = n-C_8H_{17}$ ,  $C_6H_5$ , p-tolyl, p-bromophenyl, o-hydroxyphenyl) using the Ahn adduct **9** as stoichiometric oxygen source.

highly efficient for the oxidative esterification in combination with Ahn adducts. Lewis acids such as  $\rm ZnBr_2$  and LiI, have been tested as catalysts under various conditions, however, carboxylic acid was always obtained as a main product. It should be noted that the acid also forms slowly when the nonyl aldehyde is exposed to the atmosphere. In case the reactions are performed under air for ten minutes or one hour in the presence of 10 mol%  $\rm AlCl_3$  as the catalyst, 69% and 91% conversion are achieved with mostly carboxylic acid as the product, while the ester content was only 9% and 33%, respectively. Therefore, in the following all reactions were carried out under a purified nitrogen atmosphere.

It is furthermore important to maintain anhydrous conditions, as AlCl<sub>3</sub> that has been exposed to the atmosphere over prolonged times loses its activity as a Lewis acid catalyst due to hydrolysis. Broensted acids are not efficient for the esterification. For example, when aqueous HCl is used under the standard conditions described below (Table S3,† entry 6), conversion to the carboxylic acid is mainly observed, with only trace amounts of ester formed. It is noteworthy that AlCl<sub>3</sub> does not hydrolyze readily in the presence of anhydrous methanol. As demonstrated by multinuclear NMR earlier the adduct [AlCl<sub>2</sub>(MeOH)<sub>4</sub>]<sup>+</sup> forms.<sup>75</sup> Fortunately, due to their high solubilities in organic solvents, Ahn adducts do not require reaction mixtures to be aqueous or biphasic systems, which expands their applications to include water sensitive compounds and materials such as AlCl<sub>3</sub> in organic and inorganic synthesis. The water formed during the oxidation reaction remains bound to the phosphine oxide carrier. 11,41,47,48

Tables 6 and S3† summarize the effects of the oxidant, the catalyst and the reaction time on the outcome of the direct esterification of nonyl aldehyde. When the reaction is carried out under the standard conditions (1 equiv. aldehyde, 0.6 equiv. of 9 and 0.25 equiv. of AlCl<sub>3</sub>) for ten minutes, about 72% conversion with 80% ester in the product mixture are observed (entry 1). At a longer reaction time of 45 minutes, nearly quantitative conversion could be achieved and the ester was generated selectively (entry 2). Control experiments were performed without the catalyst, without the oxidant, and without both. Only about 12%, 13%, and 4% conversion were obtained, with carboxylic acid being the dominant product (Table 6,

Table 6 Direct oxidative esterification of 1 equivalent of nonyl aldehyde using the Ahn adduct  $Ph_3PO\cdot(HOO)_2CMe_2$  (9) as oxygen source and  $AlCl_3$  as the catalyst

Entry	Adduct (equiv.)	Catalyst (equiv.)	Time (min)	Main product	Conversion (%)	Ester in product (%)
1	0.60	0.25	10	Ester	71.7	80
2	0.57	0.25	45	Ester	99.6	100
3	0.60	0	45	Acid	11.6	0
4	0	0.26	45	Acid	12.6	32
5	0	0	45	Acid	3.9	0

All reactions have been performed in 1 mL of methanol and at room temperature under a nitrogen atmosphere.

entries 3, 4, and 5). The nature of the di(hydroperoxy)alkane adducts is uncritical, for example, application of adducts 2–4 as oxidizers under the standard conditions lead to comparable esterification results.

In Tables 7 and S4† the effect of the oxidizer amount on the esterification reaction is summarized. In all Ahn adducts, there are two peroxide groups per phosphine oxide carrier, which can potentially oxidize the aldehyde to the ester in the presence of the alcohol. It has been demonstrated earlier that Ahn adducts lose active oxygen atoms in a stepwise manner, with the second peroxo group per adduct assembly being more reluctant to release the oxygen. 53,54 In order to clarify whether both peroxo groups of an Ahn adduct are used for the oxidative esterification, or only one, a series of reactions using different amounts of adduct 9 has been performed under the standard conditions (Table 7). When about 1.2 molar equivalents of 9 are applied, meaning a peroxo oxygen content of about 2.1 equivalents, nearly quantitative conversion to form the ester selectively is observed (97.4%, entry 1). Reducing the amount of 9 to ca. 0.6 eq., which still amounts to a peroxo oxygen content of about 0.96 equivalents per aldehyde, still 99.6% conversion has been achieved, again with selective ester formation (entry 2). This result shows unequivocally that both peroxide groups in 9 were consumed in the oxidation reaction. It should be noted that no carboxylic acid has been found in the reaction mixtures.

To further corroborate the result that both peroxide groups in 9 were used for the oxidation, substoichiometric amounts of the adduct were employed (Table 7, entries 3 and 4). About 0.4 and 0.3 equivalents of the adduct, corresponding to active oxygen contents of *ca.* 0.7 and 0.5 equivalents per aldehyde

**Table 7** Direct oxidative esterification of 1 equivalent of nonyl aldehyde using the Ahn adduct  $Ph_3PO\cdot(HOO)_2CMe_2$  (9) as oxygen source and  $AlCl_3$  as the catalyst

Entry		Active oxygen (equiv.)	Catalyst (equiv.)	Conversion (%)	Ester in product (%)
1	1.21	2.06	0.27	97.4	100
2	0.57	0.96	0.25	99.6	100
3	0.39	0.67	0.25	83.8	100
4	0.27	0.46	0.26	58.7	100

All reactions have been performed in 1 mL of methanol and at room temperature under a nitrogen atmosphere. The reaction time was 45 minutes for all entries.

group were applied. Hereby, about 84% and 59% conversion were achieved with 100% ester selectivity in each case. These conversion values relate to the expected values of 67% and 46%, assuming that the active oxygen atoms in both peroxo groups of the adduct performed the oxidation. Therefore, we can conclude that both peroxide groups in the Ahn adduct were used for the direct oxidative esterification of the nonyl aldehyde.

In order to test the range of applicable substrates, the more demanding aromatic substrates benzaldehyde (10), the electron rich p-methylbenzaldehyde (11) and the electron deficient p-bromobenzaldehyde (12), as well as the intramolecularly hydrogen-bonded o-hydroxybenzaldehyde (13) were subjected to the standard procedure over different amounts of time. The results of the unoptimized reactions are summarized in Tables 8, S5, and S6.† All reactions yielded the corresponding ester as the main product.

For benzaldehyde, a conversion of 32% was found after only 45 minutes. A longer reaction time of 6 hours with the same amounts of catalyst and oxidizer led to much higher conversion of nearly 80%. An 86% conversion of 10 to 100% ester can alternatively be achieved by doubling the amount of 9 and AlCl<sub>3</sub> (Table 8).

Similarly, the more electron rich 11 requires a longer reaction time of 5 hours for 70% conversion under otherwise standard conditions of 0.6 and 0.3 equivalents of oxidizer and catalyst (Table 8). The example of 12 shows that a bromine substituent at the phenyl ring can be tolerated under the standard

Table 8 Direct oxidative esterification of 1 equivalent each of benzaldehyde (10), p-methylbenzaldehyde (11), p-bromobenzaldehyde (12), and o-hydroxybenzaldehyde (13) using the Ahn adduct Ph<sub>3</sub>PO·(HOO)<sub>2</sub>CMe<sub>2</sub> (9) as oxygen source and AlCl<sub>3</sub> as the catalyst

Aldehyde	Adduct (equiv.)	Catalyst (equiv.)	Time	Conversion (%)	Ester in product (%)
10	0.59	0.26	45 min	32.1	100
10	1.05	0.46	5 h	85.6	100
10	0.60	0.25	6 h	79.2	95.5
11	0.62	0.27	45 min	37.2	93
11	0.62	0.27	5 h	70.0	88
12	0.67	0.26	5 h	82.1	100
13	0.65	0.24	5 h	45.6	100

All reactions have been performed in 1 mL of methanol and at room temperature under a nitrogen atmosphere. In each reaction the ester was the main product.

reaction conditions and within 5 hours a conversion of 82% with optimal selectivity of 100% was obtained. For the aromatic substrate 13 with an intramolecular hydrogen bridge between the OH group in *ortho* position and the aldehyde oxygen, a reaction time of 5 hours results in *ca.* 46% conversion and the product consists only of the ester (Table 8).

# 3. Conclusions

Four new di(hydroperoxy)adamantane adducts 1-4 have been synthesized. One adduct features hydrogen-bound water (1), the others (2-4) are Ahn adducts with the corresponding phosphine oxides p-Tol<sub>2</sub>P=O (5), o-Tol<sub>2</sub>P=O (6), and  $Cv_3$ P=O (7). Furthermore, an unexpected dimeric reaction product (8) of 1,2,5-phenylphosphole is reported. It is demonstrated that the adducts can be synthesized easily, and with reproducible composition. All adducts 1-4 and 8 are characterized by single crystal X-ray diffraction. For the di(hydroperoxy)adamantane adducts 2-4 one general structural motif is identified. In the context of earlier studies of our group and others, the presented work highlights the interesting structural diversity and reactivity of the P=O···H assembly. The <sup>31</sup>P, <sup>13</sup>C, and <sup>1</sup>H NMR data of 2-4 are analyzed and compared to the parent phosphine oxides. The hydrogen bonding in 1-4 is further confirmed by IR and Raman spectroscopy. It is demonstrated that Ahn adducts in general function as efficient oxygen donors for the direct esterification of aldehydes. In combination with the inexpensive and readily available Lewis acid catalyst AlCl<sub>3</sub> quantitative and selective conversion of nonyl aldehyde to the methyl ester is achieved at ambient temperature within 45 minutes. Hereby, the active oxygen atoms of both peroxo groups in the Ahn adduct are consumed for the direct oxidative esterification. The more challenging aromatic aldehydes benzaldehyde (10), p-methylbenzaldehyde (11) p-bromobenzaldehyde (12), and o-hydroxybenzaldehyde (13) can selectively be transformed into the esters in high yields by increasing the reaction times to 5 hours or alternatively by doubling the amounts of oxidizer and catalyst.

In future work phosphines and phosphine oxides will be covalently  $^{35,36}$  or electrostatically  $^{35d,76}$  bound to silica. Immobilized Ahn adducts can subsequently be obtained by reaction with aqueous  $H_2O_2$  in the presence of ketones. Immobilization will allow the easy separation of the phosphine oxide carrier from the esterification reaction mixture and its regeneration and reuse by adding  $H_2O_2$  and ketones. The covalently anchored phosphine oxides and their peroxo adducts can be characterized with classical solid-state NMR  $^{35,36,39-41,76}$  in the dry state and HRMAS in the presence of a solvent.  $^{35d,b,e,f,36}$ 

# 4. Experimental section

#### (a) General considerations

All reactions were carried out using standard Schlenk line techniques and a purified  $N_2$  atmosphere, if not stated otherwise.

Reagents purchased from Sigma Aldrich or VWR were used without further purification. Aqueous  $H_2O_2$  solution (35% w/w) was obtained from Acros Organics and used as received. Solvents were dried by boiling them over sodium, then they were distilled and stored under purified nitrogen. Acetone, dichloromethane (Aldrich, ACS reagent grade) and ethanol (200 proof) were dried over 3 Å molecular sieves (EMD Chemical Inc.) prior to use.  $AlCl_3$  was used as received from Beantown Chemical in the form of grains (anhydrous, 99% pure), and was stored under an inert atmosphere.

#### (b) NMR spectroscopy

The  $^{1}$ H,  $^{13}$ C, and  $^{31}$ P NMR spectra were recorded at 499.70, 125.66, and 202.28 MHz on a 500 MHz Varian spectrometer. The  $^{13}$ C and  $^{31}$ P NMR spectra were recorded with  $^{1}$ H decoupling if not stated otherwise. Neat Ph<sub>2</sub>PCl ( $\delta(^{31}$ P) = +81.92 ppm) in a capillary centered in the 5 mm NMR tubes was used for referencing the  $^{31}$ P chemical shifts of dissolved compounds. For referencing the  $^{1}$ H and  $^{13}$ C chemical shifts, if not mentioned otherwise, the residual proton and the carbon signals of the solvents were used ( $C_{6}D_{6}$ :  $\delta(^{1}$ H) = 7.16 ppm,  $\delta(^{13}$ C) = 128.00 ppm; CDCl<sub>3</sub>:  $\delta(^{1}$ H) = 7.26 ppm,  $\delta(^{13}$ C) = 77.00 ppm). The signal assignments were based on comparisons with analogous phosphine oxides.  $^{11,47,51-55}$ 

#### (c) IR spectroscopy

The IR spectra of the neat powders of all adducts and compounds were recorded with a Shimadzu IRAffinity-1 FTIR spectrometer equipped with a Pike Technologies MIRacle ATR plate.

### (d) Raman spectroscopy

The Raman spectra were acquired using a Jobin–Yvon Horiba Labram HR instrument coupled to an Olympus BX41 microscope with 514.51 nm laser excitation from an Arion laser. A 600 lines per mm grating and an acquisition time of 2 s were applied. 60 scans gave spectra of good quality.

#### (e) X-Ray diffraction

see ESI.†

#### (f) Synthesis and characterization

Synthesis of H<sub>2</sub>O·(HOO)<sub>2</sub>C(C<sub>9</sub>H<sub>14</sub>) (1). The water adduct 1 has been synthesized according to a literature procedure.<sup>57</sup> Adamantanone (1.00 g, 6.66 mmol) and iodine (169 mg, 0.666 mmol) are dissolved in acetonitrile (13.3 ml). Aqueous hydrogen peroxide (2.29 mL, 35%, 11.62 M, 26.6 mmol) is added and the reaction mixture is stirred for 24 h. The mixture is concentrated under reduced pressure and extracted with dichloromethane (60 mL) once. The organic phase is dried over sodium sulfate and filtered. The filtrate is concentrated under reduced pressure to *ca.* 3 mL and the product is purified by column chromatography, eluting with pentane, then dichloromethane, and finally with ethyl acetate. The water adduct of *gem*-di(hydroperoxy)adamantane 1 is obtained as a colorless solid (944 mg, 4.32 mmol, 65% yield). Melting range 90–93 °C.

NMR ( $\delta$ , CDCl<sub>3</sub>), <sup>1</sup>H 2.11–1.65 (m, 14H, H2–H5); <sup>13</sup>C{<sup>1</sup>H} 112.87 (s, C1), 35.83 (s, C2\*), 33.69 (s, C3<sup>#</sup>), 31.02 (s, C4\*), 25.94 ppm (s, C5<sup>#</sup>). \*,<sup>#</sup>assignments interchangeable. IR:  $\nu$ (O–H) = 3433 (H<sub>2</sub>O),  $\nu$ (O–H) = 3339 (OOH),  $\delta$ (O–H) = 1659 (H<sub>2</sub>O) cm<sup>-1</sup>.

Synthesis of  $p\text{-Tol}_3\text{PO-(HOO)}_2\text{C(C}_9\text{H}_{14})$  (2).  $p\text{-Tol}_3\text{PO}$  (163 mg, 0.508 mmol) and di(hydroperoxy)adamantane (102 mg, 0.508 mmol) are dissolved in dichloromethane (10 mL). Hexanes (10 mL) is added to the mixture and the solvent is allowed to evaporate. Colorless crystals (231 mg, 0.443 mmol, 87% yield) are obtained. Melting point 135–137 °C.

NMR ( $\delta$ , CDCl<sub>3</sub>), <sup>31</sup>P{<sup>1</sup>H} 32.30 (s); <sup>1</sup>H 7.52 (dd, <sup>3</sup>J(<sup>31</sup>P-<sup>1</sup>H) = 11.9 Hz, <sup>3</sup>J(<sup>1</sup>H-<sup>1</sup>H) = 8.1 Hz, 6H, H2'), 7.24 (dd, <sup>3</sup>J(<sup>1</sup>H-<sup>1</sup>H) = 7.9 Hz, <sup>4</sup>J(<sup>31</sup>P-<sup>1</sup>H) = 2.2 Hz, 6H, H3'), 2.38 (s, 9H, H5'), 2.11-1.61 (m, 14H, H2-H5); <sup>13</sup>C{<sup>1</sup>H} 142.53 (d, <sup>4</sup>J(<sup>31</sup>P-<sup>13</sup>C) = 2.8 Hz, C4'), 132.18 (d, <sup>2</sup>J(<sup>31</sup>P-<sup>13</sup>C) = 10.4 Hz, C2'), 129.32 (d, <sup>3</sup>J(<sup>31</sup>P-<sup>13</sup>C) = 12.6 Hz, C3'), 129.13 (d, <sup>1</sup>J(<sup>31</sup>P-<sup>13</sup>C) = 107.2 Hz, C1'), 111.27 (s, C1), 35.86 (s, C2\*), 33.90 (s, C3\*), 31.05 (s, C4\*), 25.95 (s, C5\*), 21.69 ppm (d, <sup>5</sup>J(<sup>31</sup>P-<sup>13</sup>C) = 1.3 Hz, C5'). \*\*\*assignments interchangeable. IR:  $\nu$ (O-H) = 3269,  $\nu$ (P=O) = 1153 cm<sup>-1</sup>.

Synthesis of  $o\text{-Tol}_3\text{PO}\cdot(\text{HOO})_2\text{C}(\text{C}_9\text{H}_{14})$  (3).  $o\text{-Tol}_3\text{PO}\cdot(160 \text{ mg}, 0.499 \text{ mmol})$  and di(hydroperoxy)adamantane (100 mg, 0.499 mmol) are dissolved in 10 mL of CH $_2\text{Cl}_2$ . Then, hexanes (10 mL) is added to the mixture and the solvent is allowed to evaporate under ambient conditions. Colorless crystals (195 mg, 0.374 mmol, 75% yield) can be isolated. Melting point 141–143 °C.

NMR ( $\delta$ , CDCl<sub>3</sub>), <sup>31</sup>P{<sup>1</sup>H} 39.87 (s); <sup>1</sup>H 7.44 (t, <sup>3</sup>J(<sup>1</sup>H-<sup>1</sup>H) = 7.5 Hz, 3H, H4'), 7.32 (dd, <sup>3</sup>J(<sup>1</sup>H-<sup>1</sup>H) = 7.4 Hz, <sup>4</sup>J(<sup>31</sup>P-<sup>1</sup>H) = 4.1 Hz,

Synthesis of  $\text{Cy}_3\text{PO}\cdot(\text{HOO})_2\text{C}(\text{C}_9\text{H}_{14})$  (4).  $\text{Cy}_3\text{PO}$  (148 mg, 0.499 mmol) and di(hydroperoxy)adamantane (100 mg, 0.499 mmol) are dissolved in methylene chloride (10 mL). After adding hexanes (10 mL), the reaction mixture is left for the solvent to slowly evaporate. Colorless crystals (199 mg, 0.400 mmol, 80% yield) are yielded. Melting point 159–161 °C.

NMR ( $\delta$ , CDCl<sub>3</sub>), <sup>31</sup>P{<sup>1</sup>H} 58.04 (s); <sup>1</sup>H 11.25 (br. s, 2H, OOH), 2.06–1.60 (m, 32H, H2–5, H1'<sub>eq</sub>, H2'<sub>eq</sub>, H3'<sub>eq</sub>, H4'<sub>eq</sub>); 1.42 (q, <sup>3</sup>J(<sup>1</sup>H–<sup>1</sup>H) = 11.2 Hz, 6H, H2'<sub>ax</sub>), 1.29–1.22 (m, 9H, H3'<sub>ax</sub>, H4'<sub>ax</sub>); <sup>13</sup>C{<sup>1</sup>H} 111.01 (s, C1), 35.89 (s, C2\*), 34.89 (d, <sup>1</sup>J(<sup>31</sup>P–<sup>13</sup>C) = 60.1 Hz, C1'), 33.99 (s, C3\*), 31.50 (s, C4\*), 27.49 (s, C5\*), 26.86 (d, <sup>3</sup>J(<sup>31</sup>P–<sup>13</sup>C) = 12.0 Hz, C3'), 26.15 (d, <sup>2</sup>J(<sup>31</sup>P–<sup>13</sup>C) = 3.0 Hz, C2'), 26.05 ppm (d, <sup>4</sup>J(<sup>31</sup>P–<sup>13</sup>C) = 1.2 Hz, C4'). \*,\*\*assignments interchangeable. IR:  $\nu$ (O–H) = 3225 cm<sup>-1</sup>,  $\nu$ (P=O) = 1101 cm<sup>-1</sup>.

Synthesis of phosphole oxide dimer dichloromethane adduct (8). 1,2,5-Triphenylphosphole (400 mg, 1.28 mmol) is dissolved in 14 mL of  $\mathrm{CH_2Cl_2}$ . Hydrogen peroxide (6 mL, 50%, 17.6 M, 105.6 mmol) is added and the biphasic mixture is stirred vigorously (1150 rpm). The phases are separated and 5 mL of hexanes is added to the organic phase. After slow evaporation of the solvent, the yellow precipitate is washed with pentane (2  $\times$  5 mL). The solid is recrystallized from a 1:1 mixture of dichloromethane with hexanes by slow evaporation of the solvents. A yellow crystalline material (414.2 mg, 0.558 mmol, 87% yield) is collected.

#### (g) Standard procedure for oxidative direct esterification

In a representative experiment, a Schlenk flask was charged with anhydrous AlCl<sub>3</sub> (10.1 mg, 0.0757 mmol) under nitrogen. Then, dry, degassed CH<sub>3</sub>OH (1.0 mL, 25 mmol) was added to the Schlenk flask. Finally, Ph<sub>3</sub>PO·(HOO)<sub>2</sub>CMe<sub>2</sub> (9) (65.9 mg, 0.171 mmol) and nonyl aldehyde (43.0 mg, 0.302 mmol) were added and the reaction mixture was stirred for 45 min under nitrogen. Next, methanol was evaporated *in vacuo* and the

remaining viscous liquid was used for obtaining the aldehyde conversion and potential product ratios by  $^1H$  NMR. The yield of crude ester was determined as 99.6% based on the presence of the dominant triplet of the  $\alpha\text{-CH}_2$  protons of the methyl nonanoate at 2.30 ppm and the low intensity triplet of the  $\alpha\text{-CH}_2$  protons of the nonyl aldehyde at 2.41 ppm.

#### (h) Procedure for isolating methyl nonanoate

Anhydrous AlCl<sub>3</sub> (59.8 mg, 0.450 mmol) was weighed into a Schlenk flask and dissolved in dry, degassed CH<sub>3</sub>OH (10.0 mL, 248 mmol) under nitrogen. Subsequently, Ph<sub>3</sub>PO·(HOO)<sub>2</sub>CMe<sub>2</sub> (9) (889.8 mg, 2.303 mmol) and nonyl aldehyde (250.0 mg, 1.760 mmol) were added and the reaction mixture was stirred for 45 min. Then 0.50 mL of liquid was removed from the reaction mixture, methanol was removed in vacuo, and the remaining viscous liquid was used for obtaining the aldehyde conversion and potential product ratios by <sup>1</sup>H NMR. The yield of crude ester was determined as 100% based on the sole presence of the triplet peak of the α-CH<sub>2</sub> protons of the methyl nonanoate at 2.30 ppm. Next, all methanol was removed from the remaining reaction mixture in the Schlenk flask under high vacuum. Then 37 mL of hexanes were added to extract the organic products. The resulting suspension was stirred for 20 minutes and left overnight for the precipitate to settle. Next, the solution was transferred to another Schlenk flask via filtration through a cotton plug. The hexanes were removed in vacuo and the remaining liquid was recondensed. Methyl nonanoate was obtained as a colorless liquid with the characteristic fruity odor (109.6 mg, 0.6372 mmol, 38% isolated yield, not optimized). The NMR data of methyl nonanoate are in agreement with the literature.<sup>77</sup> <sup>1</sup>H NMR (CDCl<sub>3</sub>):  $\delta$  = 3.66 (s, 3H), 2.30 (t, 2H), 1.61 (quint, 2H), 1.28 (m, 10 H), 0.87 (t, 3H); <sup>13</sup>C{<sup>1</sup>H} NMR (CDCl<sub>3</sub>):  $\delta$  = 174.49, 51.63, 34.28, 31.95, 29.36, 29.30, 29.25, 25.11, 22.78, 14.23 ppm.

# Conflicts of interest

There are no conflicts of interest to declare.

# Acknowledgements

This work was supported by the National Science Foundation (CHE-1900100). We thank Dr Jordon W. Benzie for performing experiments for the Ahn adduct formation with secondary phosphines.

# Notes and references

1 (a) D. Duprey and F. Cavani, Handbook of Advanced Methods and Processes in Oxidation Catalysis, Imperial College Press, 2014; (b) F. Cavani and J. H. Teles, Sustainability in Catalytic Oxidation: An Alternative Approach or a Structural Evolution?, ChemSusChem, 2009, 2, 508-534; (c) A. E. Comyns, Peroxides and Peroxide Compounds, in

Van Nostrand's Encyclopedia of Chemistry, John Wiley & Sons, Inc., 2005.

- 2 A. G. Medvedev, A. V. Churakov, P. V. Prikhodchenko, O. Lev and M. V. Vener, Crystalline Peroxosolvates: Nature of the Coformer, Hydrogen-Bonded Networks and Clusters, Intermolecular Interactions, *Molecules*, 2021, 26, 26.
- 3 (a) C. J. Legacy, A. Wang, B. J. O'Day and M. H. Emmert, Iron-Catalyzed  $C_{\alpha}$ -H Oxidation of Tertiary, Aliphatic Amines to Amides under Mild Conditions, *Angew. Chem., Int. Ed.*, 2015, **54**, 14907–14910; (b) C. J. Legacy and M. H. Emmert,  $C_{\alpha}$ -H Oxidations of Amines to Amides: Expanding Mechanistic Understanding and Amine Scope through Catalyst Development, *Synlett*, 2016, **27**, 1893–1897.
- 4 (a) D. J. Covell and M. C. White, A C-H Oxidation Approach for Streamlining Synthesis of Chiral Polyoxygenated Motifs, *Tetrahedron*, 2013, 69, 7771–7778; (b) P. E. Gormisky and M. C. White, Catalyst-Controlled Aliphatic C-H Oxidations with a Predictive Model for Site-Selectivity, *J. Am. Chem. Soc.*, 2013, 135, 14052–14055; (c) T. J. Osberger, D. C. Rogness, J. T. Kohrt, A. F. Stepan and M. C. White, Oxidative Diversification of Amino Acids and Peptides by Small-Molecule Iron Catalysis, *Nature*, 2016, 537, 214–219; (d) J. M. Howell, K. Feng, J. R. Clark, L. J. Trzepkowski and M. C. White, Remote Oxidation of Aliphatic C-H Bonds in Nitrogen-Containing Molecules, *J. Am. Chem. Soc.*, 2015, 137, 14590–14593.
- 5 (a) J. Hou, Y. Chen, B. Cordes, D. Ma, J. Wang, X. Wang, F. E. Kühn, H. Guo and M. D. Zhou, Methyltrioxorhenium-Catalyzed Highly Selective Dihydroxylation of 1,2-Allenylic Diphenyl Phosphine Oxides, Chem. Commun., 2015, 51, 7439-7442; (b) M. D. Zhou, M. Liu, J. Huang, J. Zhang, J. Wang, X. Li, F. E. Kühn and S. L. Zang, Olefin Epoxidation with Hydrogen Peroxide using Octamolybdate-Based Self-Separating Catalysts, Green Chem., 2015, 17, 1186-1193; (c) M. Drees, S. A. Hauser, M. Cokoja and F. E. Kühn, DFT Studies on the Reaction Pathway of the Catalytic Olefin Epoxidation with CpMoCF<sub>3</sub> Dioxo and Oxo-Peroxo Complexes, J. Organomet. Chem., 2013, 748, 36-45; (d) M. A. Goodman and M. R. Detty, Selenoxides as Catalysts for Epoxidation and Baeyer-Villiger Oxidation with Hydrogen Peroxide, Synlett, 2006, 1100-1104; (e) I. I. E. Markovits, W. A. Eger, S. Yue, M. Cokoja, C. J. Münchmeyer, B. Zhang, M.-D. Zhou, A. Genest, J. Mink, S.-L. Zang, N. Rösch and F. E. Kühn, Activation of Hydrogen Peroxide by Ionic Liquids: Mechanistic Studies and Application in the Epoxidation of Olefins, Chem. - Eur. J., 2013, 19, 5972-5979; (f) H. Yao and D. E. Richardson, Epoxidation of Alkenes with Bicarbonate-Activated Hydrogen Peroxide, J. Am. Chem. Soc., 2000, 122, 3220-3221; (g) G. S. Owens and M. M. Abu-Omar, Methyltrioxorhenium-Catalyzed Epoxidations in Ionic Liquids, Chem. Commun., 2000, 1165-1166.
- 6 (a) P. C. B. Page, B. R. Buckley, C. Elliott, Y. Chan, N. Dreyfus and F. Marken, Chemoselective Oxidation of Sulfides to Sulfoxides with Urea-Hydrogen Peroxide Complex Catalysed by Diselenide, *Synlett*, 2016, 27, 80–82;

- (b) D. Habibi, M. A. Zolfigol, M. Safaiee, A. Shamsian and A. Ghorbani-Choghamarani, Catalytic Oxidation of Sulfides to Sulfoxides using Sodium Perborate and/or Sodium Percarbonate and Silica Sulfuric Acid in the Presence of 2009, Catal. Commun., 10, 1257-1260; (c) H. Golchoubian and F. Hosseinpoor, Effective Oxidation of Sulfides to Sulfoxides with Hydrogen Peroxide under Transition-Metal-Free Conditions, Molecules, 2007, 12, 304-311; (d) M. Amini, M. Bagherzadeh, Z. Moradi-Shoeili, D. M. Boghaei, A. Ellern and L. K. Woo, Selective Oxidation of Sulfides and Olefins by a Manganese(III) Complex Containing an N,O-type Bidentate Oxazine Ligand, I. Coord. Chem., 2013, 66, 464-472; (e) T. Okada, H. Matsumuro, S. Kitagawa, T. Iwai, K. Yamazaki, Y. Kinoshita, Y. Kimura and M. Kirihara, Selective Synthesis of Sulfoxides through Oxidation of Sulfides with Sodium Hypochlorite Pentahydrate Crystals, Synlett, 2015, 26, 2547-2552; (f) J.-W. Chu and B. L. Trout, On the Mechanism of Oxidation of Organic Sulfides by H<sub>2</sub>O<sub>2</sub> in Aqueous Solutions, J. Am. Chem. Soc., 2004, 126, 900-908; (g) E. Wojaczynska and J. Wojaczynski, Enantioselective Synthesis of Sulfoxides, Chem. Rev., 2010, 110, 4303-4356.
- 7 (a) D. W. Stephan, The Broadening Reach of Frustrated Lewis Pair Chemistry, *Science*, 2016, 354, 1248;
  (b) J. M. Bayne and D. W. Stephan, Phosphorus Lewis Acids: Emerging Reactivity and Applications in Catalysis, *Chem. Soc. Rev.*, 2016, 45, 765–774.
- 8 M. Mehta, I. G. De la Arada, M. Perez, D. Porwal, M. Oestreich and D. W. Stephan, Metal-Free Phosphine Oxide Reductions Catalyzed by  $B(C_6F_5)_3$  and Electrophilic Fluorophosphonium Cations, *Organometallics*, 2016, 35, 1030–1035.
- 9 Z. S. Han, N. Goyal, M. A. Herbage, J. D. Sieber, B. Qu, Y. Xu, Z. Li, J. T. Reeves, J.-N. Desrosiers, S. Ma, N. Grinberg, H. Lee, H. P. R. Mangunuru, Y. Zhang, D. Krishnamurthy, B. Z. Lu, J. J. Song, G. Wang and C. H. Senanayake, Efficient Asymmetric Synthesis of P-Chiral Phosphine Oxides via Properly Designed and Activated Benzoxazaphosphinine-2-Oxide Agents, J. Am. Chem. Soc., 2013, 135, 2474–2477.
- 10 T. E. Barder and S. L. Buchwald, Rationale behind the Resistance of Dialkylbiaryl Phosphines toward Oxidation by Molecular Oxygen, J. Am. Chem. Soc., 2007, 129, 5096–5101.
- 11 C. R. Hilliard, N. Bhuvanesh, J. A. Gladysz and J. Blümel, Synthesis, Purification, and Characterization of Phosphine Oxides and Their Hydrogen Peroxide Adducts, *Dalton Trans.*, 2012, 41, 1742–1754.
- 12 (a) M. Uyanik and K. Ishihara, Baeyer-Villiger Oxidation Using Hydrogen Peroxide, ACS Catal., 2013, 3, 513–520;
  (b) L. Zhou, X. Liu, J. Ji, Y. Zhang, X. Hu, L. Lin and X. Feng, Enantioselective Baeyer-Villiger Oxidation: Desymmetrization of Meso Cyclic Ketones and Kinetic Resolution of Racemic 2-Arylcyclohexanones, J. Am. Chem. Soc., 2012, 134, 17023–17026; (c) L. Zhou, X. Liu, J. Ji, Y. Zhang, W. Wu, Y. Liu, L. Lin and X. Feng, Regio- and Enantioselective Baeyer-Villiger Oxidation: Kinetic

- Resolution of Racemic 2-Substituted Cyclopentanones, *Org. Lett.*, 2014, **16**, 2938–3941.
- 13 K. Ekoue-Kovi and C. Wolf, One-Pot Oxidative Esterification and Amidation of Aldehydes, *Chem. Eur. J.*, 2008, **14**, 6302–6315.
- 14 N. Mori and H. Togo, Facile oxidative conversion of alcohols to esters using molecular iodine, *Tetrahedron*, 2005, 61, 5915–5925.
- 15 (*a*) A. Nishihara and I. J. Kubota, Oxidation of aldehyde in alcoholic media with the Caro acid, *Org. Chem.*, 1968, 33, 2525–2526; (*b*) B. R. Travis, M. Sivakumar, O. Hollist and B. Borhan, Facile Oxidation of Aldehydes to Acids and Esters with Oxone, *Org. Lett.*, 2003, 5, 1031–1034.
- 16 N. N. Karade, V. H. Budhewar, A. N. Katkar and G. B. Tiwari, Oxidative methyl esterification of aldehydes promoted by molecular and hypervalent (III) iodine, *ARKIVOC*, 2006, 2006, 162–167.
- 17 (a) C. McDonald, H. Holcomb, K. Kennedy, E. Kirkpatrick, T. Leathers and P. Vanemon, The N-iodosuccinimide-mediated conversion of aldehydes to methyl esters, *J. Org. Chem.*, 1989, 54, 1213–1215; (b) D. Minato, Y. Nagasue, Y. Demizu and O. Onomura, Effecient Kinetic Resolution of Racemic Amino Aldehydes by Oxidation with N-Iodosuccinimide, *Angew. Chem., Int. Ed.*, 2008, 47, 9458–9461; (c) Y.-F. Chenung, N-bromosuccinimide: direct oxidation of aldehydes to acid bromides, *Tetrahedron Lett.*, 1979, 20, 3809–3810; (d) I. E. Markó, A. Mekhalfia and W. D. Ollis, Radical Mediated Oxidations in Organic Chemistry: 2. The Direct Preparation of Esters from Aldehydes, *Synlett*, 1990, 347–348.
- 18 (*a*) R. V. Stevens and K. T. Chapman, Further studies on the utility of sodium hypochlorite in organic synthesis. Selective oxidation of diols and direct conversion of aldehydes to esters, *Tetrahedron Lett.*, 1982, 23, 4647–4650.
- 19 S. Sayama and T. Onami, Esterification of Aldehydes and Alcohols with Pyridinium Hydrobromide Perbromide in Water, *Synlett*, 2004, 2739–2745.
- 20 R. Tank, U. Pathak, M. Vimal, S. Bhattacharyya and L. K. Pandey, Hydrogen peroxide mediated efficient amidation and esterification of aldehydes: Scope and selectivity, *Green Chem.*, 2011, 13, 3350–3354.
- 21 R. Grigg, T. R. B. Mitchell and S. Sutthivaiyakit, Oxidation of alcohols by transition metal complexes—iv: The rhodium catalysed synthesis of esters from aldehydes and alcohols, *Tetrahedron*, 1981, 37, 4313–4319.
- 22 (a) R. Gopinath and B. K. A. Patel, Catalytic Oxidative Esterification of Aldehydes Using V<sub>2</sub>O<sub>5</sub>–H<sub>2</sub>O<sub>2</sub>, *Org. Lett.*, 2000, 2, 577–579; (b) R. Gopinath, B. Barkakaty, B. Talukdar and B. K. Patel, Peroxovanadium-Catalyzed Oxidative Esterification of Aldehydes, *J. Org. Chem.*, 2003, 68, 2944–2947; (c) D. Talukdar, K. Sharma, S. K. Bharadwaj and A. J. Thakur, VO(acac)<sub>2</sub>: An Efficient Catalyst for the Oxidation of Aldehydes to the Corresponding Acids in the Presence of Aqueous H<sub>2</sub>O<sub>2</sub>, *Synlett*, 2013, 24, 963–966.
- 23 (a) R. Lerebours and C. Wolf, Chemoselective Nucleophilic Arylation and Single-Step Oxidative Esterification of

Aldehydes Using Siloxanes and a Palladium—Phosphinous Acid as a Reaction Switch, *J. Am. Chem. Soc.*, 2006, **128**, 13052–13053; (*b*) C. Liu, L. Zheng, D. Liu, H. Zhang and A. Lei, Covalently Bound Benzyl Ligand Promotes Selective Palladium—Catalyzed Oxidative Esterification of Aldehydes with Alcohols, *Angew. Chem., Int. Ed.*, 2012, **51**, 5662–5666; (*c*) B. A. Taschaen, J. R. Schmink and G. A. Molander, Pd-Catalyzed Aldehyde to Ester Conversion: A Hydrogen Transfer Approach, *Org. Lett.*, 2013, **15**, 500–503.

- 24 (a) C. Marsden, E. Taarning, D. Hansen, L. Johansen, S. K. Klitgaard, K. Egeblad and C. H. Christensen, Aerobic oxidation of aldehydes under ambient conditions using supported gold nanoparticle catalysts, *Green Chem.*, 2008, 10, 168–170; (b) K. Suzuki, T. Yamaguchi, K. Matsushita, C. Iitsuka, J. Miura, T. Akaogi and H. Ishida, Aerobic Oxidative Esterification of Aldehydes with Alcohols by Gold-Nickel Oxide Nanoparticle Catalysts with a Core-Shell Structure, *ACS Catal.*, 2013, 3, 1845–1849.
- 25 X.-F. Wu and C. Darcel, Iron-Catalyzed One-Pot Oxidative Esterification of Aldehydes, *Eur. J. Org. Chem.*, 2009, 1144–1147.
- 26 (a) W.-J. Yoo and C.-J. Li, Copper-catalyzed oxidative esterification of alcohols with aldehydes activated by Lewis acids, *Tetrahedron Lett.*, 2007, 48, 1033–1035; (b) Y. Zhu and Y. Wei, Copper-catalyzed oxidative esterification of aldehydes with dialkyl peroxides: efficient synthesis of esters of tertiary alcohols, *RSC Adv.*, 2013, 3, 13668–13670.
- (a) B. E. Maki and K. A. Scheidt, N-Heterocyclic, Carbene-Catalyzed Oxidation of Unactivated Aldehydes to Esters, Org. Lett., 2008, 10, 4331–4334; (b) S. De Sarkar, S. Grimme and A. Studer, NHC Catalyzed Oxidations of Aldehydes to Esters: Chemoselective Acylation of Alcohols in Presence of Amines, J. Am. Chem. Soc., 2010, 132, 1190–1191; (c) E. E. Finney, K. A. Ogawa and A. J. Boydston, Organocatalyzed Anodic Oxidation of Aldehydes, J. Am. Chem. Soc., 2012, 134, 12374–12377.
- (a) M. Zhang, S. Zhang, G. Zhang, F. Chen and J. Cheng, Palladium/NHC-catalyzed oxidative esterification of aldehydes with phenols, *Tetrahedron Lett.*, 2011, 52, 2480–2483;
  (b) J. Zhao, C. Much-Lichtenfeld and A. Studer, Cooperative N–Heterocyclic Carbene (NHC) and Ruthenium Redox Catalysis: Oxidative Esterification of Aldehydes with Air as the Terminal Oxidant, *Adv. Synth. Catal.*, 2013, 355, 1098–1106.
- 29 (a) N. V. Klassen, D. Marchington and H. C. E. McGowan, H<sub>2</sub>O<sub>2</sub> Determination by the I<sub>3</sub><sup>-</sup> Method and by KMnO<sub>4</sub> Titration, Anal. Chem., 1994, 66, 2921–2925; (b) Y. Cui, B. Zhang, B. Liu, H. Chen, G. Chen and D. Tang, Sensitive Detection of Hydrogen Peroxide in Foodstuff using an Organic-Inorganic Hybrid Multilayer-Functionalyzed Graphene Biosensing Platform, Microchim. Acta, 2011, 174, 137–144.
- 30 (a) L. Ji, Y.-N. Wang, C. Qian and X.-Z. Chen, Nitrile-Promoted Alkene Epoxidation with Urea-Hydrogen Peroxide (UHP), *Synth. Commun.*, 2013, 43, 2256–2264; (b) D. Kaur and B. R. Chhabra, Silica Supported Urea-

- Hydrogen Peroxide as a Source of Oxygen, J. Chem. Biol., Phys. Sci. A, 2013, 3, 980-987; (c) M. C. Ball and S. Massey, The Thermal Decomposition of Solid Urea Hydrogen Peroxide, Thermochim. Acta, 1995, 261, 95-106; (d) J. A. Dobado, J. Molina and D. Portal, Theoretical Study on the Urea-Hydrogen Peroxide 1:1 Complexes, J. Phys. Chem. A, 1998, 102, 778-784; (e) S. Taliansky, Urea-Hydrogen Peroxide Complex, Synlett, 2005, 1962-1963; (f) M. S. Cooper, H. Heaney, A. J. Newbold and W. R. Sanderson, Oxidation Reactions Using Urea-Hydrogen Peroxide; A Safe Alternative to Anhydrous Hydrogen Peroxide, Synlett, 1990, 533-535.
- 31 (a) N. Koukabi, Sodium Percarbonate: A Versatile Oxidizing Reagent, *Synlett*, 2010, 2969–2970; (b) A. McKillop and W. R. Sanderson, Sodium Perborate and Sodium Percarbonate: Further Applications in Organic Synthesis, *J. Chem. Soc., Perkin Trans.* 1, 2000, 471–476; (c) D. P. Jones and W. P. Griffith, Alkali-metal Peroxocarbonates, M<sub>2</sub>[CO<sub>3</sub>]·nH<sub>2</sub>O<sub>2</sub>, M<sub>2</sub>[C<sub>2</sub>O<sub>6</sub>], M[HCO<sub>4</sub>]·nH<sub>2</sub>O, and Li<sub>2</sub>[CO<sub>4</sub>]·H<sub>2</sub>O, *J. Chem. Soc., Dalton Trans.*, 1980, 2526–2532.
- 32 A. V. Arzumanyan, R. A. Novikov, A. O. Terent'ev, M. M. Platonov, V. G. Lakhtin, D. E. Arkhipov, A. A. Korlyukov, V. V. Chernyshev, A. N. Fitch, A. T. Zdvizhkov, I. B. Krylov, Y. V. Tomilov and G. I. Nikishin, Nature Chooses Rings: Synthesis of Silicon-Containing Macrocyclic Peroxides, *Organometallics*, 2014, 33, 2230–2246, and refs. cited.
- 33 S. Kharel, T. Jia, N. Bhuvanesh, J. H. Reibenspies, J. Blümel and J. A. Gladysz, A Non-templated Route to Macrocyclic Dibridgehead Diphosphorus Compounds: Crystallographic Characterization of a Crossed-Chain Variant of *in/out* Stereoisomers, *Chem. Asian J.*, 2018, **13**, 2632–2640.
- 34 (a) J. Chrzanowski, D. Krasowska and J. Drabowicz, Synthesis of Optically Active Tertiary Phosphine Oxides: A Historical Overview and the Latest Advances, Heteroat. Chem., 2018, 29, e21476; (b) T. Kovacs and G. Keglevich, The Reduction of Tertiary Phosphine Oxides by Silanes, Curr. Org. Chem., 2017, 21, 569-585; (c) D. Herault, D. H. Nguyen, D. Nuel and G. Buono, Reduction of Secondary and Tertiary Phosphine Oxides to Phosphines, Chem. Soc. Rev., 2015, 44, 2508-2528; (d) M. D. Fletcher, Organophosphorus Reagents, 2004, 171-214; (e) H. R. Hays and D. J. Peterson, Org. Phosphorus Compd., 1972, 3, 341-500; (f) H. Adams, R. C. Collins, S. Jones and C. J. A. Warner, Enantioselective Preparation of P-Chiral Phosphine Oxides, Org. Lett., 2011, 13, 6576-6579; (g) K. C. K. Swamy, N. N. B. Kumar, E. Balaraman and K. V. P. P. Kumar, Mitsunobu and Related Reactions: Advances and Applications, Chem. Rev., 2009, 109, 2551-2651; (h) R. H. Beddoe, K. G. Andrews, V. Magne, J. D. Cuthbertson, J. Saska, A. L. Shannon-Little, S. E. Shanahan, H. F. Sneddon and R. M. Denton, Redox-Neutral Organocatalytic Misunobu Reactions, Science, 2020, **365**, 910–914; (*i*) D. W. Stephan, The Broadening Reach of Frustrated Lewis Pair Chemistry, Science, 2016, 354, 1248; (j) J. M. Bayne and D. W. Stephan, Phosphorus Lewis

Acids: Emerging Reactivity and Applications in Catalysis, *Chem. Soc. Rev.*, 2016, 45, 765–774; (*k*) X. Cai, S. Majumdar, G. C. Fortman, L. M. Frutos, M. Temprado, C. R. Clough, C. C. Cummins, M. E. Germain, T. Palluccio, E. V. Rybak-Akimova, B. Captain and C. D. Hoff, Thermodynamic, Kinetic, and Mechanistic Study of Oxygen Atom Transfer from Mesityl Nitrile Oxide to Phosphines and to a Terminal Metal Phosphido Complex, *Inorg. Chem.*, 2011, **50**, 9620–9630.

- 35 Selected references: (a) J. Blümel, Linkers and Catalysts Immobilized on Oxide Supports: New Insights by Solid-State NMR Spectroscopy, Coord. Chem. Rev., 2008, 252, 2410-2423; (b) J. Guenther, J. Reibenspies and J. Blümel, Synthesis, Immobilization, CP- and HR-MAS NMR of a New Chelate Phosphine Linker System, and Catalysis by Rhodium Adducts thereof, Adv. Synth. Catal., 2011, 353, 443-460; (c) R. Silbernagel, A. Diaz, E. Steffensmeier, Clearfield and J. Blümel, Wilkinson-type Hydrogenation Catalysts Immobilized on Zirconium Phosphate Nanoplatelets, J. Mol. Catal. A: Chem., 2014, **394**, 217–223; (*d*) J. H. Baker, N. Bhuvanesh and J. Blümel, Tetraphosphines with Tetra(biphenyl)silane -Stannane Cores as Rigid Scaffold Linkers for Immobilized Catalysts, J. Organomet. Chem., 2017, 847, 193-203; (e) J. C. Pope, T. Posset, N. Bhuvanesh and J. Blümel, The Palladium Component of an Immobilized Sonogashira Catalyst System: New Insights Multinuclear HRMAS NMR Spectroscopy, Organometallics, 2014, 33, 6750-6753; (f) T. Posset, J. Guenther, J. Pope, T. Oeser and J. Blümel, Immobilized Sonogashira Catalyst Systems: New Insights by Multinuclear HRMAS NMR Chem. Commun., 2011, 47, 2059–2061; (g) K. J. Cluff, N. Bhuvanesh and J. Blümel, Monometallic Ni(0) and Heterobimetallic Ni(0)/Au(1) Complexes of Tripodal Phosphine Ligands: Characterization in Solution and in the Solid State and Catalysis, Chem. - Eur. J., 2015, 21, 10138-10148.
- 36 J. Guenther, J. Reibenspies and J. Blümel, Synthesis and Characterization of Tridentate Phosphine Ligands Incorporating Long Methylene Chains and Ethoxysilane Groups for Immobilizing Molecular Rhodium Catalysts, *Mol. Catal.*, 2019, 479, 110629.
- 37 (a) A. Zheng, S.-B. Liu and F. Deng, <sup>31</sup>P NMR Chemical Shifts of Phosphorus Probes as Reliable and Practical Acidity Scales for Solid and Liquid Catalysts, *Chem. Rev.*, 2017, 117, 12475–12531; (b) R. Yerushalmi, J. C. Ho, Z. Fan and A. Javey, Phosphine Oxide Monolayers on SiO<sub>2</sub> Surfaces, *Angew. Chem., Int. Ed.*, 2008, 47, 4440–4442; (c) J. P. Osegovic and R. S. Drago, Measurement of the Global Acidity of Solid Acids by <sup>31</sup>P MAS NMR of Chemisorbed Triethylphosphine Oxide, *J. Phys. Chem. B*, 2000, 104, 147–154; (d) S. Hayashi, K. Jimura and N. Kojima, Adsorption of Trimethylphosphine Oxide on Silicalite Studied by Solid-State NMR, *Bull. Chem. Soc. Jpn.*, 2014, 87, 69–75; (e) S. Machida, M. Sohmiya, Y. Ide and Y. Sugahara, Solid-State <sup>31</sup>P Nuclear Magnetic Resonance

Study of Interlayer Hydroxide Surfaces of Kaolinite Probed with an Interlayer Triethylphosphine Oxide Monolayer, *Langmuir*, 2018, **34**, 12694–12701.

- 38 (a) A. R. Wilmsmeyer, W. O. Gordon, E. D. Davis, B. A. Mantooth, T. A. Lalain and J. R. Morris, Multifunctional Ultra-High Vacuum Apparatus for Studies of the Interactions of Chemical Warfare Agents on Complex Surfaces, *Rev. Sci. Instrum.*, 2014, 85, 014101; (b) J. Kemsley, Studying Warfare Agents Directly, *Chem. Eng. News*, 2014, 92, 29–30.
- 39 P. J. Hubbard, J. W. Benzie, V. I. Bakhmutov and J. Blümel, Disentangling Different Modes of Mobility of Triphenylphosphine Oxide Adsorbed on Alumina, *J. Chem. Phys.*, 2020, **152**, 054718.
- 40 S. Kharel, K. J. Cluff, N. Bhuvanesh, J. A. Gladysz and J. Blümel, Structures and Dynamics of Secondary and Tertiary Alkylphosphine Oxides Adsorbed on Silica, *Chem. Asian J.*, 2019, **14**, 2704–2711.
- 41 C. R. Hilliard, S. Kharel, K. J. Cluff, N. Bhuvanesh, J. A. Gladysz and J. Blümel, Structures and Unexpected Dynamic Properties of Phosphine Oxides Adsorbed on Silica Surfaces, *Chem. Eur. J.*, 2014, **20**, 17292–17295.
- 42 (*a*) A. E. Stross, G. Iadevaia and C. A. Hunter, Cooperative Duplex Formation by Synthetic H-Bonding Oligomers, *Chem. Sci.*, 2016, 7, 94–101; (*b*) G. Iadevaia, A. E. Stross, A. Neumann and C. A. Hunter, Mix and Match Backbones for the Formation of H-Bonded Duplexes, *Chem. Sci.*, 2016, 7, 1760–1767; (*c*) R. Cuypers, E. J. R. Sudhölter and H. Zuilhof, Hydrogen Bonding in Phosphine Oxide/Phosphate–Phenol Complexes, *ChemPhysChem*, 2010, 11, 2230–2240.
- 43 D. Nunez-Villanueva and C. A. Hunter, Homochiral Oligomers with Highly Flexible Backbones from Stable H-Bonded Duplexes, *Chem. Sci.*, 2017, **8**, 206–213.
- 44 N. A. Bewick, A. Arendt, Y. Li, S. Szafert, T. Lis, K. A. Wheeler, J. Young and R. Dembinski, Synthesis and Solid-State Structure of (4-Hydroxy-3,5-diiodophenyl)phosphine Oxides. Dimeric Motifs with the Assistance of O-H···O=P Hydrogen Bonds, *Curr. Org. Chem.*, 2015, **19**, 469–474.
- 45 S. J. Pike and C. A. Hunter, Fluorescent and Colorimetric Molecular Recognition Probe for Hydrogen Bond Acceptors, *Org. Biomol. Chem.*, 2017, **15**, 9603–9610.
- 46 N. J. Burke, A. D. Burrows, M. F. Mahon and J. E. Warren, Hydrogen Bond Network Structures Based on Sulfonated Phosphine Ligands: The Effects of Complex Geometry, Cation Substituents and Phosphine Oxidation on Guanidinium Sulfonate Sheet Formation, *Inorg. Chim. Acta*, 2006, **359**, 3497–3506.
- 47 F. F. Arp, N. Bhuvanesh and J. Blümel, Hydrogen Peroxide Adducts of Triarylphosphine Oxides, *Dalton Trans.*, 2019, 48, 14312–14325.
- 48 S. Kharel, N. Bhuvanesh, J. A. Gladysz and J. Blümel, New Hydrogen Bonding Motifs of Phosphine Oxides with a Silanediol, a Phenol, and Chloroform, *Inorg. Chim. Acta*, 2019, **490**, 215–219.

- 49 E. Y. Tupikina, M. Bodensteiner, P. M. Tolstoy, G. S. Denisov and I. G. Shenderovich, P=O Moiety as an Ambidextrous Hydrogen Bond Acceptor, *J. Phys. Chem. C*, 2018, **122**, 1711–1720.
- 50 G. Begimova, E. Y. Tupikina, V. K. Yu, G. S. Denisov, M. Bodensteiner and I. G. Shenderovich, Effect of Hydrogen Bonding to Water on the <sup>31</sup>P Chemical Shift Tensor of Phenyl- and Trialkylphosphine Oxides and α-Amino Phosphonates, *J. Phys. Chem. C*, 2016, **120**, 8717–8729.
- 51 F. F. Arp, N. Bhuvanesh and J. Blümel, Di(hydroperoxy) cycloalkane Adducts of Triarylphosphine Oxides: A Comprehensive Study Including Solid-State Structures and Association in Solution, *Inorg. Chem.*, 2020, 59, 13719–13732.
- 52 F. F. Arp, S. H. Ahn, N. Bhuvanesh and J. Blümel, Selective Synthesis and Stabilization of Peroxides via Phosphine Oxides, *New J. Chem.*, 2019, 43, 17174–17181.
- 53 S. H. Ahn, K. J. Cluff, N. Bhuvanesh and J. Blümel, Hydrogen Peroxide and Di(hydroperoxy)propane Adducts of Phosphine Oxides as Stoichiometric and Soluble Oxidizing Agents, *Angew. Chem.*, 2015, 127, 13539–13543, (*Angew. Chem. Int. Ed.*, 2015, 54, 13341–13345).
- 54 S. H. Ahn, N. Bhuvanesh and J. Blümel, Di(hydroperoxy) alkane Adducts of Phosphine Oxides: Safe, Solid, Stoichiometric, and Soluble Oxidizing Agents, *Chem. Eur. J.*, 2017, 23, 16998–17009.
- 55 S. H. Ahn, D. Lindhardt, N. Bhuvanesh and J. Blümel, Di (hydroperoxy)cycloalkanes Stabilized via Hydrogen Bonding by Phosphine Oxides: Safe and Efficient Baeyer-Villiger Oxidants, ACS Sustainable Chem. Eng., 2018, 6, 6829–6840.
- 56 W. Harnying, P. Sudkaow, A. Biswas and A. Berkessel, N-Heterocyclic Carbene/Carboxylic Acid Co-Catalysis Enables Oxidative Esterification of Demanding Aldehydes/ Enals, at Low Catalyst Loading, *Angew. Chem.*, 2021, **60**, 19631–19636.
- 57 K. Žmitek, M. Zupan, S. Stavber and J. Iskra, Iodine as a Catalyst for Efficient Conversion of Ketones to *gem*-Dihydroperoxides by Aqueous Hydrogen Peroxide, *Org. Lett.*, 2006, **8**, 2491–2494.
- 58 The following CCDC reference numbers contain the supplementary crystallographic data for the corresponding species 1–5 for this paper: CCDC 1980801 (H<sub>2</sub>O·(HOO)<sub>2</sub>C (C<sub>9</sub>H<sub>14</sub>), 1), 1980802 (*p*-Tol<sub>3</sub>PO·(HOO)<sub>2</sub>C(C<sub>9</sub>H<sub>14</sub>), 2), 1980803 (*o*-Tol<sub>3</sub>PO·(HOO)<sub>2</sub>C(C<sub>9</sub>H<sub>14</sub>), 3), 1980804 (Cy<sub>3</sub>PO·(HOO)<sub>2</sub>C(C<sub>9</sub>H<sub>14</sub>), 4), 2023784 (phosphole dimer dichloromethane adduct, 8).†
- 59 F. R. Fronczek, CCDC 1021095, CSD Communication, 2014. DOI: 10.5517/cc138jkg.†
- 60 J. A. Davies, S. Dutremez and A. Pinkerton, A. Solid-state phosphorus-31 NMR and X-ray crystallographic studies of tertiary phosphines and their derivatives, *Inorg. Chem.*, 1991, 30, 2380–2387.

61 G. A. Jeffrey, *An Introduction to Hydrogen Bonding*, Oxford University Press, Oxford, 1997.

- 62 E. N. Baker and R. E. Hubbard, Hydrogen Bonding in Globular Proteins, *Prog. Biophys. Mol. Biol.*, 1984, **44**, 97–179.
- 63 N. De Silva, F. Zahariev, B. P. Hay, M. S. Gordon and T. L. Windus, *J. Phys. Chem. A*, 2015, **119**, 8765–8773.
- 64 T. J. Barton and A. J. Nelson, *Tetrahedron Lett.*, 1969, 57, 5037–5040.
- 65 A. G. Dikundwar, P. Chodon, S. P. Thomas and H. Bhutani, *Cryst. Growth Des.*, 2017, 17, 1982–1990.
- 66 (a) M. Korb, S. W. Lehrich and H. Lang, J. Org. Chem., 2017, 82, 3102–3124; (b) P. A. Shaw, G. J. Clarkson and J. P. Rourke, Chem. Sci., 2017, 8, 5547–5558; (c) K. Fujimoto and A. Osuka, Chem. Sci., 2017, 8, 8231–8239; (d) M. Yamamura, T. Saito and T. Nabeshima, J. Am. Chem. Soc., 2014, 136, 14299–14306.
- 67 H. Günzler and H.-U. Gremlich, *IR-Spektroskopie*, Wiley-VCH, 4th edn, 2003.
- 68 T. Tsuneda, J. Miyake and K. Miyatake, Mechanism of  $\rm H_2O_2$  Decomposition by Triphenylphosphine Oxide, *ACS Omega*, 2018, 3, 259–265.
- 69 W. H. Fletcher and J. S. Rayside, High resolution vibrational Raman spectrum of oxygen, *J. Raman Spectrosc.*, 1974, 2, 3–14.
- 70 M. Hayyan, M. A. Hashim and I. M. AlNashef, Superoxide Ion: Generation and Chemical Implications, *Chem. Rev.*, 2016, 116, 3029–3085.
- 71 R. C. Taylor and P. C. Cross, Raman Spectra of Hydrogen Peroxide in Condensed Phases. I. The Spectra of the Pure Liquid and Its Aqueous Solutions, *J. Chem. Phys.*, 1956, 24, 41–44.
- 72 P. A. Giguére and T. K. K. Srinivasan, A Raman study of  $H_2O_2$  and  $D_2O_2$  vapor, *J. Raman Spectrosc.*, 1974, 2, 125–132.
- 73 H. H. Eysel and S. Thym, RAMAN Spectra of Peroxides, *Z. Anorg. Allg. Chem.*, 1975, **411**, 97–102.
- 74 V. Vacque, B. Sombret, J. P. Huvenne, P. Legrand and S. Suc, Characterisation of the O-O peroxide bond by vibrational spectroscopy, *Spectrochim. Acta, Part A*, 1997, 53, 55–66.
- 75 J. W. Akitt and R. H. Duncan, Christine Setchell, Multinuclear (<sup>1</sup>H, <sup>27</sup>Al, and <sup>35(</sup>Cl) Nuclear Magnetic Resonance Studies of Solutions of Aluminium Salts in Methanol, Aqueous Methanol, and Aqueous Acetone, J. Chem. Soc., Dalton Trans., 1983, 2639–2643.
- 76 Y. Yang, B. Beele and J. Blümel, Easily Immobilized Di- and Tetraphosphine Linkers: Rigid Scaffolds that Prevent Interactions of Metal Complexes with Oxide Supports, *J. Am. Chem. Soc.*, 2008, **130**, 3771–3773.
- 77 M. Amezquita-Valencia and G. Achonduh, Pd-Catalyzed Regioselective Alkoxycarbonylation of 1–Alkenes Using a Lewis Acid [SnCl<sub>2</sub> or Ti(O<sup>i</sup>Pr)<sub>4</sub>] and a Phosphine, H. Alper, J. Org. Chem., 2015, 80, 6419–6424.